Iris Model Based on Local Orientation Description

Junzhou Huang, Li Ma, Yunhong Wang, Tieniu Tan,

National Laboratory of Pattern Recognition (NLPR),
Institute of Automation, Chinese Academy of Sciences, Beijing, P.R. China, 100080
{jzhuang, lma, wangyh, tnt}@nlpr.ia.ac.cn

Abstract

In recent years, iris recognition has received increasing attention due to its distinct characteristics. This paper proposes a new approach to iris recognition based on local orientation description. In this approach, a bank of Log-Gabor filters are used to capture local orientation characteristics of the iris so as to produce discriminating features. Experimental results show that the proposed method has an encouraging performance and indicate that differences of local details among irises can be well characterized by local orientation information.

Keywords: *Iris recognition, Local orientation, Log-Gabor, Biometrics*

1. Introduction

Iris can be used to identify persons and has recently received increasing attention due to its distinct characteristics [1-3]. The human iris, an annular part between the black pupil and the white sclera as shown in Figure 1(a), has many interlacing minute characteristics such as freckles, coronas, stripes, furrows, crypts and so on. Generally, the characteristics of the iris spread along the radial direction in the original image. Therefore, the discriminability information of the iris is higher in the angular direction.

So far, no method only utilizes orientation information to characterize an iris. However, our intuitive observations about the orientation characteristics of the iris show that local orientation information is also abundant and random in iris texture. Especially, this randomness makes orientation possible to be discriminating features for recognition. Therefore, it is still a puzzle if orientation based iris feature representation can achieve high recognition performance. In order to explore this puzzle, a new feature extraction algorithm only based on local orientation is proposed for recognition in this paper.

The remainder of this paper is organized as follows. Related work is presented in Section 2. Section 3 describes the details of the orientation based iris feature extraction method. It includes three main steps, namely preprocessing, feature extraction, matching. Extensive experimental results are presented and discussed in Section 4. Section 5 concludes this paper.

2. Related work

Daugman developed iris identification software and published his wonderful results in 1993 [4]. Later, similar work has been investigated, such as Wildes' [12][13], Boles' [14], Lim's [15] and Tan's [16-19] systems, which differ either in the iris feature representations or pattern matching algorithms. The state of the art of iris recognition is glanced as follows.

Daugman [4][5][10] used multi-scale Gabor wavelets to extract phase structure information of the iris texture. By the above operations, he acquired a 2048-bit iris-code and compared the difference between a pair of iris representations by computing their Hamming distance via the XOR operator. From his work, we cannot judge whether orientation information is useful for recognition. Wildes et al. [6] used a Hough transform for iris localization, then applied Laplacian pyramid (multi-scale decomposition) to represent distinctive spatial characteristics of iris. Unlike Daugman, Wildes chose the modified normalized correlation for matching. Boles and Boashah [7] built one-dimensional representation for various resolution levels of a co-centric circle on the iris. Then, 1-D wavelet transform with four levels was used to characterize the spatial variations of the iris. Iris matching was based on two dissimilarity functions. The randomness of orientation is not effectively used in their method. Lim et al. [8] exploited 2-D Harr wavelet transform to extract high frequency information of iris to form an 87-bit code and implemented the classification using a modified competitive learning neural network. In [9], Tan et al. developed an efficient algorithm for iris recognition by characterizing key local variations. The basic idea was that local sharp variation points, denoting the appearing or vanishing of an important image structure, were utilized to represent the shape of randomly distributed blocks of the iris. The whole procedure of feature extraction included two steps: 1) A set of one-dimensional (1-D) intensity signals was constructed to effectively characterize the most important information of the original two-dimensional (2-D) images; 2) Using a particular class of wavelets, a sequence of positions of local sharp variation points in such signals was recorded as features.

3. Our approach

The human iris patterns have distinct characteristics of epigenetic randomness, complexity and singularity [10], which make iris have abundant texture information. It is vital for an iris recognition method to be able to accurately represent these characteristics. From the viewpoint of texture analysis, the local spatial patterns in an iris mainly involve frequency and orientation information. Until now, most researchers on iris recognition used frequency information for recognition. However, no attempt to the best of our knowledge is made to use orientation as features for recognition. As discussed above, intuitive observations enable us to suppose that local orientation may be a good

feature for recognition. Here, we propose a feature extraction method based on local orientation of iris. It includes iris image preprocessing, local orientation feature extraction and matching.

3.1 Iris image preprocessing

An iris image (shown in Figure 1a,) contains not only the region of iris but also eyelid, pupil, etc. Furthermore, the intensity of an iris image is not uniformly distributed because of illumination variations. To reduce the influence of these factors and facilitate the subsequent processing, the original iris images should be preprocessed before feature extraction. The preprocessing mainly includes three steps, namely localization, normalization and enhancement. More details of preprocessing may be found in [9]. Figure 1 shows an example of iris image preprocessing.

(a)   (b)

(c)

(d)
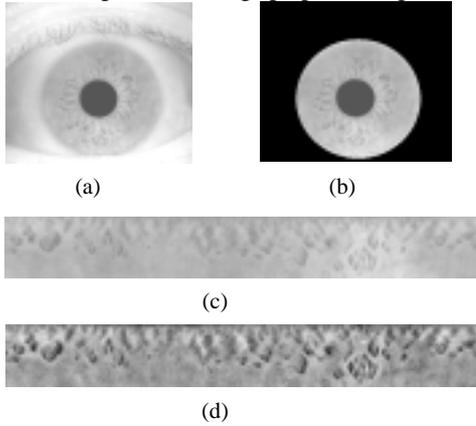
Figure 1. *Preprocessing (a) Original iris image, (b) localized image, (c) Normalized image, (d) Enhanced image*

3.2 Local orientation feature extraction

Similar to the method described in [12][13], a bank of Log-Gabor filters are adopted to represent local orientation characteristics of the iris.

3.2.1 Log-Gabor filter

Recently, Log-Gabor filter has been widely used in computer vision, especially for texture analysis [11-16]. Field and Kovesi conclude that the Log-Gabor function more closely reflects the frequency response for the task of analyzing natural images and is consistent with measurement of the mammalian visual system [12-14].

The 2D Log-Gabor filter is constructed in the frequency domain and only can be numerically constructed in the spatial domain via the inverse Fourier transform. It comprises two components, namely the radial filter component and the angular filter component. The radial filter has the transfer function:

$$G(\omega) = \exp(\frac{-(\log(\omega/\omega_0))^2}{2(\log(k/\omega_0))^2}) \qquad (1)$$

where ω_0 represents the center frequency of the filter, and k determines the bandwidth of the filter in the radial direction. The angular filter has the Gaussian transfer function:

$$G(\theta) = \exp(\frac{-(\theta-\theta_0)^2}{2T(\Delta\theta)^2}) \qquad (2)$$

where θ_0 represents the orientation angle of the filter, and T is a scaling factor, and $\Delta\theta$ is the orientation spacing between the filters.

The Log-Gabor filters are obtained by multiplying the radial and angular components together. Figure 2 shows two even and odd symmetric Log-Gabor filters with different bandwidths all tuned to the same center frequency. Each even and odd symmetric pair of Log-Gabor filters comprises a complex Log-Gabor filter at one scale.

A bank of Log-Gabor filters in 6 orientations is used in this paper. Six filter orientations can provide a good compromise between achieving an even spectral coverage and minimizing the number of orientations.

(a)   (b)
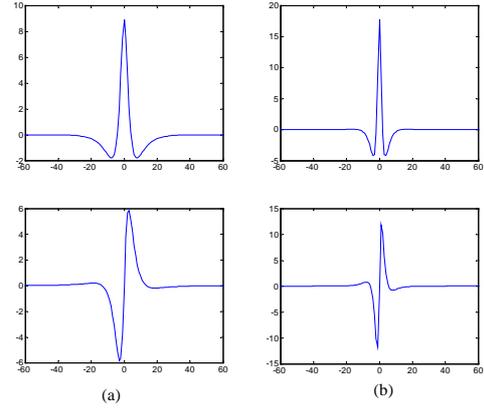
Figure 2. *Two quadrature pairs of log-Gabor* wavelets *having bandwidths of 1 and 2 octaves respectively*

3.2.2 Local orientation and feature vector

The local orientation is defined as the orientation in which the energy of the filtered image is maximal among all possible orientation energy (in this paper, 6 possible orientations, 0ο, 30ο, 60ο, 90ο, 120ο, 150ο). In order to obtain local orientation for a preprocessed iris image $I(x, y)$, orientation energy must firstly be computed. A bank of Log-Gabor filters with 6 orientations is constructed as discussed above. M_n^e and M_n^o respectively denote the even-symmetric and odd-symmetric Log-Gabor at an orientation *n* (Note that *n* has 6 possible values). A response vector is obtained from the response of each quadrature pair of filters. It is denoted as follows:

$$[e_n(x, y), o_n(x, y)] = [I(x, y)*M_n^e, I(x, y)*M_n^o] \qquad (3)$$

where * denotes convolution operator. At each point in an image, we will have six vectors respectively corresponding to each orientation of filter. These response vectors then form the basis for computing orientation energy. Therefore, the orientation energy E (x, y, n) of a point (x, y) in the orientation n is represented as follows:

$$E(x, y, n) = \sqrt{e_n^2(x, y) + o_n^2(x, y)} \qquad (4)$$

As discussed above, there are 6 orientation values for each point in the image. The local orientation of a point (x, y) is then presented as follows (Here, n $\in$ {0ο, 30ο, 60ο, 90ο, 120ο, 150ο}):

$$O(x, y) = \arg\max_n E(x, y, n) \qquad (5)$$

According to the local orientation, we can code the iris image:

$$C(x, y) = O(x, y) / 180 \qquad (6)$$

The codes are concatenated row by row to form a 1-D feature vector:

$$C = \{C_1, C_2, \cdots, C_i, \cdots, C_N\} \qquad (7)$$

where C_i denotes the features from the ith point in the image, N is the total number of points in the image.

To reduce the space dimension and the subsequent computational complexity, we down-sample each filtered image by a pair of factors $[d_x, d_y]$ before the concatenation. Here, down-sampling means replacing each (d_x x d_y) filtered block elements with their average orientation value. In our experiments, the feature vector consists of 1280 components.

3.3 Matching

For simplicity, iris matching is based on computing the Euclidean distance (ED) between the corresponding feature vectors. The ED is defined in the following:

$$ED(k) = \frac{1}{N} \sum_{i=1}^{N} (f_i^k - f_i)^2 \qquad (8)$$

where N is the dimension of the feature vector, f_i is the ith feature component of an unknown sample, f_i^k is the ith feature component of the ith class.

The nearest neighbor classifier is used in this paper. Features of an unknown iris are compared with those of irises in database. It is identified as the iris class indexed by k if the Euclidean distance defined above is a minimum at k and this minimum is also less than a reasonable threshold. No doubt, a more sophisticated classifier could be employed, but the interest here is to evaluate the genuine discriminatory ability of the extracted features.

In our algorithm, feature extraction from preprocessed iris images brings intrinsic invariance to translation and approximate scale invariance. To achieve approximate rotation invariance, we define seven templates that denote the seven rotation angles for each iris class in the database. For preprocessed iris images, these shift length values are –18, –12, –6, 0, 6, 12, 18, which approximately correspond to rotate the original iris by –12o, –8o, –4o, 0o, 4o, 8o, 12o respectively. When matching the input feature vector with the templates of a class, the minimum of the seven matching values is taken as the final matching distance.

4. Experiments

We perform extensive experiments to verify the effectiveness of the proposed algorithm. The details of the experiments are described as follows.

4.1 Data acquisition

Unlike fingerprint and face, there is currently no common iris database of a reasonable size. A new iris database, called CASIA iris dataset, is established for our experiments. The image set includes a total number of 2096 iris images from 210 subjects (to the best of our knowledge, this is the largest iris database available in the public domain). These images are captured by a digital optical sensor and can be divided into two parts. One is our earlier image set containing 500 images from 25 different people. Each individual provides 20 images (10 for each eye). These images are captured in a reasonable time interval. In the first stage, five images of each eye are acquired. Four weeks later, five more images of each eye are taken. The other part contains 1596 images from 185 subjects, which form 253 iris classes (note that not each individual provides iris images of both eyes, but at least 5 images for each eye). These images are also captured in two stages, similar to the acquisition process of the earlier image set. The total number of iris classes is thus 303 (2x25+253). Capturing images on different time provides a challenge to our algorithm. Some samples from the CASIA Iris Dataset are shown in Figure 3. The proposed algorithm is tested in two modes: 1) identification (i.e., one-to-many mode) and 2) verification (i.e., one-to-one mode). For each iris class, we randomly choose two samples as templates and the rest serves as test samples.
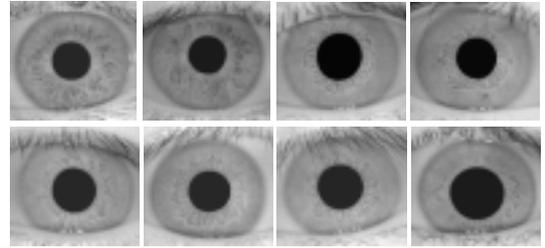
Figure 3. *Iris samples from the CASIA Iris Set*

4.2 Recognition results

We conduct a series of experiments on the CASIA Iris Set to assess the accuracy of the proposed algorithm.

4.2.1 Different down-sampling factors

The down-sampling pair $[d_x, d_y]$ introduced in section 3.2.2 has important effects on the performance of the proposed algorithm. In order to find a tradeoff between accuracy and computational complexity, we do experiments on the integrated feature vector with different down-sampling vectors. From the recognition results shown in Table 1, we can see that the performance differences are not very significant when the dimensionality of features is no less than 80, whereas when the dimensionality of features is 20, the recognition rate descends dramatically. For maintaining a good tradeoff between accuracy and computational complexity, we use 1280 features in the next series of experiments.

4.2.2 Performance of the proposed algorithm

To evaluate the accuracy of the proposed algorithm here, we test the proposed algorithm in two modes, namely identification and verification. In identification tests, our algorithm obtained a correct recognition rate of 100%. The verification results are shown in Figure 5. In particular, when the probability of false match is 1/100,000, the false rejection rate is only 1.13%.

Table1. *Recognition results using different down-sampling factor vectors*

Down-sampling vectors	Recognition rates	Dimensionality of features
[2, 4]	100%	2560
[2, 8]	100%	1280
[4, 8]	99.46%	640
[4, 16]	98.81%	320
[8, 16]	97.82%	160
[8, 32]	94.54%	80
[8, 64]	86.34%	40
[8, 128]	62.29%	20

From Figure 4, we can find that the distance between intra-class and inter-class distribution is large. This fact indicates that orientation features used in our algorithm have good discriminability.
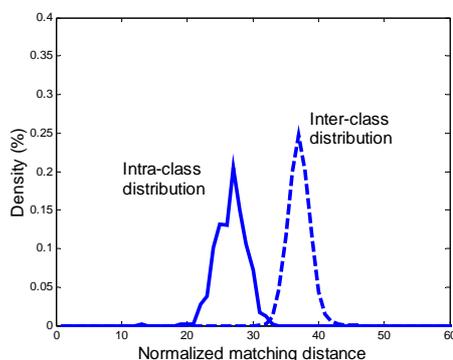
Figure 4. *Distribution of intra / inter -class distance*

Figure 5 is a false match rate (FMR) against false non-match rate (FNMR) curve [3]. This curve generally measures the accuracy of matching. The FMR is the probability that an imposter is accepted as an authorized subject. The FNMR is the probability that an authorized subject is incorrectly rejected. Points on the curve denote all possible states in different tradeoffs. The ideal FMR vs FNMR curve is a horizontal straight line with zero false non-match rate. From Figure 5, we can know that the equal error rate (EER) is about 0.06%. For a recognition algorithm, the EER is a good indicator of its recognition performance. It is the point where the false match and false non-match rate are equal. The smaller the EER is, the better the algorithm.

All above experimental results are highly encouraging. They demonstrate that our iris feature representation based on local orientation is very effective, and local orientation can indeed be used as discriminating features for iris recognition.

4.3 Comparison

There are many algorithms for iris recognition so far. Daugman's method is the most distinct in the field of iris recognition. Commercial success also confirms its high performance. From our previous work [9], we can know that Daugman's method also has better performance than others on CASIA iris database. The recognition performance of our previous method [9] is shoulder by shoulder with that of Daugman's method [5], but outperforms others. Because two methods discussed above

have best performance in CASIA iris set [9], we will make detailed comparison between our proposed method and them to prove the effectiveness of local orientation based iris feature extraction. Note that Daugman's algorithm used in the following experiments is our implementation according to the open literature [5]. Table 3 tabulates the identification results, and Figure 5 describes the verification results.

Table 3. *Comparative identification results of different methods*

Method	Correct recognition rate (%)
Daugman [5]	100
Tan [9]	100
Proposed	100
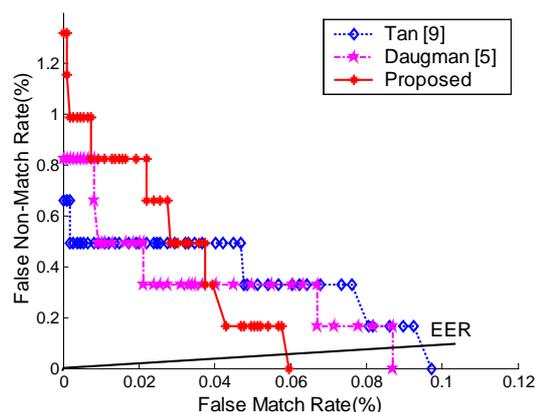
Figure 5. *Comparison of verification results*

From the results shown in Table 3 and Figure 5, we can see that the proposed method has a high performance, which is close with that of our previous method [9]. On the other hand, the equal error rate of the proposed method is relatively less than that of our previous method. In our previous work [9], a particular class of 1D dyadic wavelets is presented for characterizing key local variations so as to represent the shape of randomly distributed blocks of the iris. The orientation information is not used for representing the randomness of the iris. On the contrary, the proposed method only uses local orientation information for representing the random characteristics of the iris.

The method by Daugman [5] has a good performance, which is very close with that of the proposed method. However, it should be noted that these two methods explore different schemes to represent an iris. We represent local characteristics of the iris from the viewpoint of local orientation description, whereas Daugman used phase information to characterize the spatial variations of the iris. The dimension of feature vector is 2048 in his method. Compared with it, the feature vector extracted in the proposed method contains 1280 components.

From the above experimental results and discussions, we can conclude that local orientation can also be used to represent the distinct characteristics of the iris.

4.4 Discussions

All above experimental results not only demonstrate that the proposed algorithm has an encouraging performance, but also confirm that local orientation is also an effective

iris feature for recognition. However, efforts remain to be taken to further improve its performance.

1) The number and the class of iris samples used in our experiments are of a reasonable size. We intend to enlarge our iris database to include much more iris images from more different users so as to further evaluate the performance of the proposed algorithm.

2) Dimensionality of iris features has important effects on the performance of the proposed algorithm. Smaller dimensionality of iris features results in lower accuracy but lower computational complexity. Whereas, larger dimensionality of iris features leads to higher accuracy but higher computational complexity. Our experimental results have demonstrated that the proposed approach can obtain a tradeoff between accuracy and computational complexity when the dimensionality of iris features is 1280.

3) As far as iris recognition is concerned, feature representation methods should effectively characterize the local variations of the iris. Like Daugman's method [5] and our previous method [9], local orientation description based feature extraction in this paper also achieves good results. As our experimental results show, local orientation features can reveal the local variations of the iris and thus play an important role in iris recognition.

4) So far, no method for iris recognition has effectively explored both frequency information and orientation information for iris feature representation. Actually, combining the two useful information may lead to the improvement of iris recognition accuracy. It will be investigated in our future work.

5. Conclusions

In this paper, we have described a new method for personal identification using iris patterns. Unlike the existing methods for iris recognition, the proposed method characterizes the details of the iris from the viewpoint of local orientation description. To effectively describe the randomness of the iris, a bank of Log-Gabor filters is used to capture local orientation characteristics of the iris. The nearest center classifier is adopted for classification. The proposed algorithm can achieve a high recognition rate of 100% on a set of 2,096 images. Especially, when the probability of false match is 1/100,000, the false rejection rate is only 1.13%. Extensive experiment results have demonstrated that orientation information is also an effective feature.

Acknowledgements

References

[1] A.K. Jain, R.M. Bolle and S. Pankanti, Eds., *Biometrics: Personal Identification in a Networked Society*, Norwell, MA: Kluwer, 1999.

[2] D. Zhang, *Automated Biometrics: Technologies and Systems*, Norwell, MA: Kluwer, 2000.

[3] T. Mansfield, G. Kelly, D. Chandler and J. Kane, *Biometric Product Testing Final Report, issue 1.0*, National Physical Laboratory of UK, 2001.

[4] J.G. Daugman, "High Confidence Visual Recognition of Persons by a Test of Statistical Independence", *IEEE Trans. Pattern Analysis and Machine Intelligence*, Vol.15, No.11, pp.1148-1161, 1993.

[5] J.G. Daugman, "Statistical Richness of Visual Phase Information: Update on Recognizing Persons by Iris Patterns", *International Journal of Computer Vision*, Vol. 45, No. 1, pp 25-38, 2001.

[6] R.P. Wildes, "Iris Recognition: An Emerging Biometric Technology", In *Proceedings of the IEEE*, Vol.85, pp.1348-1363, 1997.

[7] W.W. Boles and B. Boashah, "A Human Identification Technique Using Images of the Iris and Wavelet Transform", *IEEE Trans. on Signal Processing*, Vol.46, pp.1185-1188, 1998.

[8] S. Lim, K. Lee, O. Byeon and T. Kim, "Efficient Iris Recognition through Improvement of Feature Vector and Classifier", *ETRI Journal*, Vol. 23, No. 2, pp61-70, 2001.

[9] L. Ma, T. Tan, Y. Wang and D. Zhang, "Efficient Iris Recognition by Characterizing Key Local Variations", *IEEE Trans. on Image Processing*. (Accepted with minor revision)

[10] J.G. Daugman, "The importance of being random: Statistical principles of iris recognition", *Pattern Recognition,* Vol. 36, No. 2, pp. 279-291, 2003.

[11] L. Haglund and D. J. Fleet, "Stable Estimation of Image Orientation", In *Proceedings of International Conference of Computer Vision*, pp. 68-72, 1994.

[12] Peter Kovesi, "Edges Are Not Just Steps", In *Proceedings of Asian Conference on Computer Vision*, Melbourne, pp. 822-827,2002.

[13] P. D. Kovesi, "Image Features from Phase Congruency", *Videre: Journal of Computer Vision Research*, Vol. 1, No. 3, pp. 1-26, Summer, 1999.

[14] D.J. Field, "Relations Between the Statistics of Natural Images and the Response Profiles of Cortical Cells", *Journal of the Optical Society of America A*, Vol. 4, pp. 2379-2394, 1987

[15] E.J. Holden and R. Owens, "Automatic Detection of Facial Points", In *Proceedings of Asian Conference on Computer Vision*, Melbourne, 2002.

[16] M. Robins, "Local Energy Feature Tracing in Digital Images and Volumes", *PhD Thesis*, Department of Computer Science and Software Engineering, The University of Western Australia, 1999.